Hydrol. Earth Syst. Sci. Discuss., doi:10.5194/hess-2017-259, 2017
Manuscript under review for journal Hydrol. Earth Syst. Sci.
Discussion started: 12 May 2017

Hydrology and Earth System Sciences
Open Access
Discussions

Multiple Causes of Nonstationarity in the Weihe Annual Low Flow Series

Bin Xiong[1], Lihua Xiong[1*], Jie Chen[1], Chong-Yu Xu[1, 2], Lingqi Li[1]

1 State Key Laboratory of Water Resources and Hydropower Engineering Science, Wuhan University, Wuhan 430072, P.R. China

2 Department of Geosciences, University of Oslo, P.O. Box 1022 Blindern, N-0315 Oslo, Norway

** Corresponding author:*

Lihua Xiong, PhD, Professor

State Key Laboratory of Water Resources and Hydropower Engineering Science

Wuhan University, Wuhan 430072, P.R. China

E-mail: xionglh@whu.edu.cn

Telephone: +86-13871078660

Fax: +86-27-68773568

Hydrol. Earth Syst. Sci. Discuss., doi:10.5194/hess-2017-259, 2017
Manuscript under review for journal Hydrol. Earth Syst. Sci.
Discussion started: 12 May 2017

Abstract:

Under the background of global climate change and local anthropogenic activities, multiple driving forces have introduced a variety of non-stationary components into low-flow series. This has led to a high demand on low-flow frequency analysis that considers nonstationary conditions for modeling. In this study, a nonstationary framework of low-flow frequency analysis has been developed on basis of the Generalized Linear Model (GLM) to consider time-varying distribution parameters. In GLMs, the candidate explanatory variables to explain the time-varying parameters are comprised of the eight measuring indices of the climate and catchment conditions in low flow generation, i.e., total precipitation (P), mean frequency of precipitation events (λ), temperature (T), potential evapotranspiration (ET), climate aridity index (AI_{ET}), base-flow index (BFI), recession constant (K) and the recession-related aridity index (AI_K). This framework was applied to the annual minimum flow series of both Huaxian and Xianyang gauging stations in the Weihe River, China. Stepwise regression analysis was performed to obtain the best subset of those candidate explanatory variables for the final optimum model. The results show that the inter-annual variability in the variables of those selected best subsets plays an important role in modeling annual low flow series. Specifically, analysis of annual minimum 30-day flow in Huaxian shows that AI_K is of the highest relative importance among the best subset of eight candidates, followed by BFI and AI_{ET}. The incorporation of multiple indices related to low-flow generation permits

tracing various driving forces. The established link in nonstationary analysis will be beneficial to predict future occurrences of low-flow extremes in similar areas.

Keywords: Climate Change; Streamflow Recession; Multiple Factors; Nonstationarity; Low-flow Frequency Analysis;

1. Introduction

Low flow is defined as 'flow of water in a stream during prolonged dry weather' (WMO, 1974). Yu et al. (2014) described a low flow event as a segment of hydrograph during a period of dry weather with discharge values below a preset (relatively small) threshold. According to WMO (2009), annual minimum flows averaged over several days can be used to measure low flows. The investigation of the magnitude and frequency of low flows is of primary importance for engineering design and water resources management (Smakhtin, 2001). For recent years, low flows, as an important part of river flow regime, have been attracting the increasing attentions of hydrologists and ecologists, due to the significant impacts of climate change and human activities on most functions (e.g. providing water supply for production and living, diluting waste water, ensuring navigation, meeting ecological water requirement) of river flow during low-flow periods. (Bradford and Heinonen, 2008; Du et al., 2015; Kam and Sheffield, 2015; Kormos et al., 2016; Liu et al., 2015; Sadri et al., 2015; Smakhtin, 2001; WMO, 2009).

Low flows generally originate from groundwater or other delayed outflows (Smakhtin, 2001; Tallaksen, 1995). Their generation relates to both an extended dry weather period (leading to a climatic water deficit) and complex hydrological processes which determine how these deficits propagate through the vegetation, soil and groundwater system to streamflow (WMO, 2009). Thus, not only climate conditions drivers (e.g. potential evaporation exceeds precipitation), but catchment conditions drivers (e.g. the faster hydrologic response rate to precipitation) can cause low flows. The significant factors such as precipitation, temperature, evapotranspiration, streamflow recession, large-scale teleconnections and human forces may play important roles in influencing low-flow generation (Botter et al., 2013; Giuntoli et al., 2013; Gottschalk et al., 2013; Jones et al., 2006; Kormos et al., 2016; Roderick et al., 2013; Sadri et al., 2015). Gottschalk et al. (2013) presented a derived low flow probability distribution function with climate and catchment characteristics parameters (i.e., the mean length of dry spells λ^{-1} and recession constant of streamflow K) as its distribution parameters. Botter et al. (2013) derived "a measurable index" (λ^{-1}/K) which can be used for discriminating erratic river flow regimes from persistent river flow regimes. Recently, in Van Loon and Laaha (2015) used climate and catchment characteristics (e.g. the duration of dry spells in precipitation and the base flow index) to explain the duration and deficit of hydrological drought event and offered a further understanding of low-flow generation. Those studies indicated that climate and catchment conditions play an important role in producing low flows.

In low-flow design, conventional frequency analysis estimates low-flow statistics based on recorded data with the stationary hypothesis which means that the control mechanisms of environmental factors on the generation of the hydrological variable keep invariant in the past, present and future. However, global warming and human forces have changed climate and catchment conditions in some regions. Time-varying climate and catchment conditions will create influenced low flow series The hypothesis of stationarity has been suspected (Milly et al., 2008). If this problematic method is still used, the frequency analysis will leads to high estimation error and costly design. A common method to deal with this situation is to introduce the concept of hydrologic nonstationarity into analysis and to develop appropriate nonstationary frequency analysis.

Previous hydrological literatures on frequency analysis of nonstationary low flow series mainly focus on two aspects: development of nonstationary method and exploration of covariates reflecting changing environments. Strupczewski et al. (2001) presented the method of time-varying moment which assumes that the hydrological variable of interest obeys a certain distribution type, but its moments change over time. The method of time-varying moment was modified to be the method of time-varying parameter values for the distribution representative of hydrologic data (Richard et al., 2002). Villarini et al. (2009) presented this method using the

Hydrol. Earth Syst. Sci. Discuss., doi:10.5194/hess-2017-259, 2017
Manuscript under review for journal Hydrol. Earth Syst. Sci.
Discussion started: 12 May 2017

Generalized Additive Models for Location, Scale, and Shape Parameters (GAMLSS) (Rigby and Stasinopoulos, 2005), a flexible framework to assess nonstationary time series. The time-varying parameter method can be extended to the physical covariate analysis by replacing time with any others physical covariates (Du et al., 2015; Jiang et al., 2014; Kwon et al., 2008; López and Francés, 2013; Liu et al., 2015; Villarini et al., 2010; Villarini and Strong, 2014). For example, Jiang et al. (2014) used reservoir index as explanatory variables based on the time-varying copula method for bivariate frequency analysis of nonstationary low-flow series in Hanjiang River, China. Du et al. (2015) took precipitation and air temperature as the explanatory variables to explain the inter-annual variability in low flows of Weihe River, China. Liu et al. (2015) took Sea Surface Temperature in Nino3 region, the Pacific Decadal Oscillation, the sunspot number (3 years ahead), the winter areal temperature and precipitation as the candidate explanatory variables to explain the inter-annual variability in low flows of Yichang station, China. Kam and Sheffield (2015) ascribed the increasing inter-annual variability of low flows over the eastern Unites States to North Atlantic Oscillation and Pacific North America.

Low flows are more vulnerable to influences of climate change and human activities than high flows. However, compared with the nonstationary flood frequency analysis, the studies on the nonstationary frequency analysis of low-flow series is not very extensive because of incomplete knowledge of low flow generation (Smakhtin, 2001). Most of these studies explain nonstationarity

Hydrol. Earth Syst. Sci. Discuss., doi:10.5194/hess-2017-259, 2017
Manuscript under review for journal Hydrol. Earth Syst. Sci.
Discussion started: 12 May 2017

Hydrology and Earth System Sciences
Open Access
Discussions

of low-flow series only by using climatic indicators or a single indicator of human activity. However, the indicators of catchment conditions (e.g. recession rate) related to physical hydrological process have seldom been attached in nonstationary modeling of low flow series. This leads to lack of linking with hydrological process, which in turn would exclude further analysis, such as accurately tracing origins of change in low flow series.

The goal of this study is to develop a nonstationary low-flow frequency analysis framework with the consideration of the time-varying climate and catchment conditions (TCCCs). In this framework, the climate and catchment conditions are quantified using the eight indices, i.e., meteorological variables (total precipitation P, mean frequency of precipitation events λ, temperature T and potential evapotranspiration ET), basin storage characteristics (base-flow index BFI, recession constant K) and aridity indexes (climate aridity index AI_{ET}, the recession-related aridity index AI_K). The non-stationary frequency analysis with TCCCs developed in this study is able to give the trace of nonstationary low-flow drivers and to estimate the contribution of each driver to the change in low-flow series.

This paper is organized as follows. Section 2 describes the methods. We describe the Weihe River basin and available data sets used in this study in Section 3, followed by a presentation of the results and discussion in Section 4. Section 5 summarizes the main conclusions.

Hydrol. Earth Syst. Sci. Discuss., doi:10.5194/hess-2017-259, 2017
Manuscript under review for journal Hydrol. Earth Syst. Sci.
Discussion started: 12 May 2017

2 Methodology

In this section, first, the low-flow frequency analysis model is constructed based on the nonstationary probability distributions method, in which distribution parameters serving as response variables can vary as functions of explanatory variables. Second, the candidate distributions are described to determine the different types of nonstationary frequency curves. Then, the eight candidate explanatory variables are presented to incorporate time-varying climate and catchment conditions (TCCCs) into distribution models for the nonstationary frequency analysis. Finally, estimation of model parameters and selection of models are illustrated.

2.1 Construction of the low-flow nonstationary frequency analysis model

Generally, a nonstationary frequency analysis model can be established based on the time-varying distribution parameters method (Du et al., 2015; López and Francés, 2013; Liu et al., 2015; Richard et al., 2002; Villarini and Strong, 2014). For the nonstationary probability distribution $f_Y\left(Y_t \middle| \boldsymbol{\theta}^t\right)$, let Y_t be a random variable at time t $(t = 1, 2, ..., N)$ and vector $\boldsymbol{\theta}^t = [\theta_1^t, \theta_2^t, ..., \theta_m^t]$ be the time-varying parameters. The number of parameters m in hydrological frequency analysis is generally limited to three or less. The function relationship between the k^{th} parameter θ_k^t and the multiple explanatory variables is expressed as follows:

$$g_k\left(\theta_k^t\right) = h_k\left(x_1^t, x_2^t, ..., x_n^t\right) \tag{1}$$

where $x_1^t, x_2^t, ..., x_n^t$ are explanatory variables; n is the number of explanatory variables; $g_k(\cdot)$

Hydrol. Earth Syst. Sci. Discuss., doi:10.5194/hess-2017-259, 2017
Manuscript under review for journal Hydrol. Earth Syst. Sci.
Discussion started: 12 May 2017

is the link function which ensures the compliance with restrictions on the sample space and is usually set to natural logarithm for the given negative predictions; $h_k(\cdot)$ is the function for nonstationary modeling. The theory of Generalized Linear Model (Dobson and Barnett, 2012) is used to build function relationships between distribution parameters and their explanatory variables. In GLMs, the response relationship can be generally expressed as

$$g_k\left(\theta_k^t\right) = \alpha_{0k} + \sum_{i=1}^{i=n} \alpha_{ik} x_i^t \tag{2}$$

where α_{ik} $(i = 0,1,2,...,n, k = 1,...,m)$ are the GLM parameters.

In order to give a further nonstationary analysis, Eq. (2) is modified in this study using dimensionless method. The value of θ_k^t could be assumed to be equal to its mean ($\bar{\theta}_k$) when all explanatory variables are equal to their mean ($\bar{x}_i$), i.e.,

$$\theta_k^t\left(x_1^t = \bar{x}_1, x_2^t = \bar{x}_2, ..., x_n^t = \bar{x}_n\right) = \bar{\theta}_k \tag{3}$$

Eq. (2) is then modified as

$$\begin{aligned} & g_k\left(\frac{\theta_k^t}{\bar{\theta}_k}\right) = \beta_{0k} + \sum_{i=1}^{i=n} \beta_{ik} z_i^t \\ & z_i^t = \frac{x_i^t - \bar{x}_i}{s_i}, \qquad i = 1, 2, \ldots, n \\ & \beta_{0k} = g_k\left(\frac{\theta_k^t}{\bar{\theta}_k} \middle| \theta_k^t = \bar{\theta}_k\right) = g_k(1) \end{aligned} \tag{4}$$

where z_i^t is normalized explanatory variables; s_i is the standard deviation of x_i^t; β_{ik} $(i = 1,2,...,n, k = 1,...,m)$ are the standard GLM parameters. Let the link function $g_k(\cdot)$ be the natural logarithmic function $\ln(\cdot)$ and θ_l^t be the distribution parameter in $[\theta_1^t, \theta_2^t, ..., \theta_m^t]$ with most significant change, the degree of nonstationarity in low flow series can be defined as $\ln(\theta_l^t) - \ln(\overline{\theta}_l)$. Then, the contribution c_i^t of each explanatory variable x_i^t to $\ln(\theta_1^t) - \ln(\overline{\theta}_1)$ could be defined as

$$c_i^t = \beta_{ik} \frac{x_i^t - \overline{x}_i}{s_i} \tag{5}$$

2.2 Candidate distribution functions

We need to select the form of probability distribution $f_Y(\cdot)$ to determine what type of nonstationary frequency curves will be produced. Various probability distributions have been compared or suggested in modeling of low-flow series (Du et al., 2015; Hewa et al., 2007; Liu et al., 2015; Matalas, 1963; Smakhtin, 2001). An extensive overview of distribution functions for low flow is given in Tallaksen et al. (2004). Following these recommendations, we consider five distributions, i.e. Pearson-III (PIII), Gamma (GA), Weibull (WEI), Lognormal (LOGNO) and Generalized Extremes Value (GEV) as candidates in this study (Table 1). In the case of Pearson-III distribution, considering that the parameter θ_3 of Pearson-III as lower bound should approach zero and the parameter θ_3 of GEV is quite sensitive and difficult to be estimated, we assume them to be constant in this study.

Hydrol. Earth Syst. Sci. Discuss., doi:10.5194/hess-2017-259, 2017
Manuscript under review for journal Hydrol. Earth Syst. Sci.
Discussion started: 12 May 2017

2.3 Candidate explanatory variables

We look for variables $x_1^t, x_2^t, \ldots, x_n^t$ that can explain parts of the variations in distribution parameters $\boldsymbol{\theta}^t$. From the perspective of low-flow generation, the dependency between low-flow regime and both climate and catchment conditions has been presented by previous studies (Botter et al., 2013; Gottschalk et al., 2013; Van Loon and Laaha, 2015). We focus on eight measuring indices: total precipitation, mean frequency of precipitation events, temperature, potential evapotranspiration, climate aridity index, base-flow index, recession constant and recession-related aridity index. These indices were chosen to incorporate time-varying climate and catchment conditions (TCCCs) in nonstationary modeling, of low-flow frequency and serving as candidate explanatory variables. The values of them at each year could be estimated from hydro-meteorological data. Annual precipitation (P) and temperature (T) are calculated directly by meteorological data. The remaining indices need to be estimated indirectly. Detailed estimation procedures are shown as follows.

2.3.1. Annual mean frequency of precipitation events (λ)

Annual mean frequency of precipitation events is defined as an index to represent the intensity of precipitation recharge to the streamflow:

$$\lambda = \frac{1}{W}\sum_{w=1}^{w=W}\frac{N_w(A)}{t_r} \quad (6)$$

Hydrol. Earth Syst. Sci. Discuss., doi:10.5194/hess-2017-259, 2017
Manuscript under review for journal Hydrol. Earth Syst. Sci.
Discussion started: 12 May 2017

Hydrology and Earth System Sciences
Open Access
Discussions

where $N_w(A)$ is the number of daily rainfall events A (with values more than the threshold 0.5 mm) in w^{th} windows with a length t_r; W is the number of windows.

2.3.2. Annual climate aridity index (AI_{ET})

The ratio of annual potential evaporation to precipitation, commonly known as the climate aridity index, has been used to assess the impacts of climate change on annual runoff (Arora, 2002; Jiang et al., 2015). The climate aridity index largely reflects the climatic regimes in a region and determines runoff rates (Arora, 2002). Therefore, we choose the annual climate aridity index as a measure of time-varying climate and catchment conditions and estimate its value in a whole region using

$$AI_{ET} = \frac{ET}{P} \tag{7}$$

where P is annual areal precipitation (mm); ET is annual areal potential evapotranspiration. The Hargreaves equation (Hargreaves and Samani, 1985) is applied to calculate ET using the R-package 'Evapotranspiration' (Guo, 2014).

2.3.3. Annual base-flow index (*BFI*)

The base flow index (*BFI*) is defined as the ratio of base flow to total flow. This index has been applied to quantify catchment conditions (e.g. soil, geology and storage-related descriptors) to explain hydrological drought severity (Van Loon and Laaha, 2015). We also choose annual base flow index (BFI) as a measure of TCCCs. BFI is estimated using a hydrograph separation

Hydrol. Earth Syst. Sci. Discuss., doi:10.5194/hess-2017-259, 2017
Manuscript under review for journal Hydrol. Earth Syst. Sci.
Discussion started: 12 May 2017

procedure in R-package 'lfstat' (Koffler and Laaha, 2013).

2.3.4. Annual streamflow recession constant (*K*)

Recession constant is an important catchment characteristic index measuring the time scale of the hydrological response and reflecting water retention ability in the upstream catchment (Botter et al., 2013). Various estimation methods have been developed to extract recession segments and to parameterize characteristic recession behavior of a catchment (Hall, 1968; Sawaske and Freyberg, 2014; Tallaksen, 1995).

In this study, annual recession analysis (ARA) is performed to obtain annual streamflow recession constant (*K*). In ARA, the linearized Depuit-Boussinesq equation is used to parameterize characteristic recession behavior of a catchment and is written as

$$-\frac{dQ_t}{dt} = \frac{1}{K} Q_t \tag{8}$$

where Q_t is the value at time t. Eq. (8) is investigated by plotting data points $\frac{dQ_t}{dt}$ against Q_t of all extracted recession segments from hydrographs at each year. The criteria of recession segments extraction is based on the Manual on Low-flow Estimation and Prediction (WMO, 2009). Then, the annual recession rate (K^{-1}) is estimated as the slope of fitted straight line of these data points with least square method. We calculated K using R-package 'lfstat' (Koffler and Laaha, 2013).

Hydrol. Earth Syst. Sci. Discuss., doi:10.5194/hess-2017-259, 2017
Manuscript under review for journal Hydrol. Earth Syst. Sci.
Discussion started: 12 May 2017

2.3.5. Annual recession-related aridity index (AI_K)

In this study, recession-related aridity index is defined as the ratio of recession rate (K^{-1}) to mean precipitation frequency (λ), denoted as

$$AI_K = \frac{K^{-1}}{\lambda} \tag{9}$$

This ratio plays an important role in controlling on river flow regime (Botter et al., 2013; Gottschalk et al., 2013) and serves as an indicator measuring the recession-related aridity degree of the streamflow in river channel. For example, faster recession process or lower precipitation frequency may lead to increased runoff loss or decreased precipitation supply. Consequently, the higher the value AI_K is, the more likely low flow events occur, and vice versa.

2.4 Parameter estimation

The model parameters including $\bar{\theta}_k (k=1,2,...,m)$ and β_{ik} $(i=1,2,...,n, k=1,...,m)$ are estimated. $\bar{\theta}_k (k=1,2,...,m)$ are estimated from outputs of stationary frequency analysis through maximum likelihood method. We have

$$L\left(\bar{\theta}_1,\bar{\theta}_2,...,\bar{\theta}_m\right) = \sum_{t=1}^{t=N} \ln\left[f_Y\left(y_t \middle| \bar{\theta}_1,\bar{\theta}_2,...,\bar{\theta}_m\right)\right] \tag{10}$$

where y_t is observed low flow at time t; N is the number of samples. The parameter β_{ik} $(i=1,2,...,n, k=1,...,m)$ are estimated through maximum likelihood method to produce

Hydrol. Earth Syst. Sci. Discuss., doi:10.5194/hess-2017-259, 2017
Manuscript under review for journal Hydrol. Earth Syst. Sci.
Discussion started: 12 May 2017

nonstationary low-flow frequency curves:

$$L\begin{pmatrix}\beta_{11},\ldots,\beta_{n1}\\ \ldots\\ \beta_{1m},\ldots,\beta_{nm}\end{pmatrix}=\sum_{t=1}^{t=N}\ln\left\{f_Y\left(y_t\left|\theta_1^t\left(z_1^t,\ldots,z_n^t\left|\beta_{11},\ldots,\beta_{n1}\right.\right),\ldots,\theta_m^t\left(z_1^t,\ldots,z_n^t\left|\beta_{1m},\ldots,\beta_{nm}\right.\right)\right.\right)\right\} \quad (11)$$

The residuals (normalized randomized quintile residuals) are used to test the goodness-of-fit of fitted model objects (Dunn and Symth, 1996):

$$\hat{r}_t=\Phi^{-1}\left(F_Y\left(y_t\left|\hat{\boldsymbol{\theta}}^t\right.\right)\right) \quad (12)$$

where $F_Y(\cdot)$ is the cumulative distribution of y_t; $\Phi^{-1}(\cdot)$ is the inverse function of the standard normal distribution. The distribution of the true residuals $\hat{r}_t$ converges to standard normal if the fitted model is correct. Worm plot (Buuren and Fredriks, 2001) is used to check whether $\hat{r}_t$ have a standard normal distribution.

2.5 Model selection

Model selection contains the selection of the type of probability distribution and the selection of the explanatory variables to explain the response variables (i.e., distribution parameters θ_1 and θ_2). In order to obtain the final optimal model, the selection of the explanatory variables for θ_1 and θ_2 is conducted by a stepwise selection strategies (Stasinopoulos and Rigby, 2007; Venables, 2002): select a best subset of candidate explanatory variables for θ_1 using a forward approach (which starts with no explanatory variable in the model and tests the addition of each explanatory variable using a chosen model fit criterion); given this subset for θ_1 select another subset for θ_2

(forward). The stepwise selection strategies can get a series of stepwise models with different numbers of explanatory variables. In order to detect how the number of explanatory variables influences the performance of the model for describing non-stationarity, we investigate the five types of stepwise models: the zero-covariate model or stationary model (M0), the time covariate model (M1), single physical covariate model (M2), the double physical covariate model (M3) and the optimal number physical covariate model (M4), as shown in Table 2. The model fit criterion is based on the Akaike's information criterion (Akaike, 1974) as shown by the following

$$AIC = -2ML + 2df \tag{13}$$

where ML is the log-likelihood in Eq. (11) and df is the number of degrees of freedom. The model with the lower AIC value was considered better.

3. Study Area and Data

3.1. The study area

The Weihe River, located in the southeast of the Northwest Loess Plateau, is the largest tributary of the Yellow River, China. The Weihe River has a drainage area of 134 766 km^2, covering the coordinates of $33°42'$-$37°20'$N $104°18'$-$110°37'$E (Fig. 1). This catchment generally has a semi-arid climate, with extensive sub-humid continental monsoonal influence. Average annual precipitation of the whole area over the period 1954-2009 is about 540 mm, and has a wide range (400-1000 mm) in various regions. Under the significant impacts of climate change and human activities in the Weihe River basin in recent decades, the hydrological regime of the river has changed over time (Du et al., 2015; Jiang et al., 2015; Xiong et al., 2015).

<Figure 1>

In the Weihe basin, the impacts of agricultural irrigation on runoff have been found to be significant (Jiang et al., 2015; Lin et al., 2012). Lin et al. (2012) mentioned that the annual runoff of the Weihe River was significantly affected by irrigation diversion of the Baoji Gorge irrigation area. The irrigated area of Baoji Gorge Irrigation Area increased over time since the founding of P.R. China in 1949, and due to one influential irrigation system project in that area, it became more than twice of the original one since 1971. Jiang et al. (2015) demonstrated that in the Weihe basin, irrigated area, as compared with the other indices e.g. population, gross domestic product and cultivated land area, was a more suitable human explanatory variable for explaining the time-varying behavior of annual runoff. Within the above background, it is important to considering the effects of human activities that mainly originate from irrigation diversion, and especially for studying low flow series in this basin. In this study, we use the available data (1980-2005) of the irrigation diversion system on plateau in Baoji Gorge Irrigation Area in Zhang (2008) to provide some information for the knowledge of low flow generation. The estimations of annual recession rate (K^{-1}) by the daily streamflow data are expected to incorporate the information of impacts of water diversions on the low flows in the river channel.

3.2. Streamflow data

We used daily streamflow records (1954-2009) provided by the Hydrology Bureau of the Yellow River Conservancy Commission from both Huaxian station (with a drainage area of 106 500 km^2) and Xianyang station (with a drainage area of 46 480 km^2). Low-flow extreme events were selected from the daily streamflow series using the widely-used annual minimum series method (WMO, 2009). AM_n is the annual minimum n day flow during hydrological year defined to start on 1 March. Consequently, AM_1, AM_7, AM_{15} and AM_{30} are selected as low-flow extreme events in this study. The original measure unit of streamflow data ($\mathrm{m}^3 \cdot \mathrm{s}^{-1}$) is converted to $10^{-4}\ \mathrm{m}^3 \cdot \mathrm{s}^{-1} \cdot \mathrm{km}^{-2}$ by dividing by the corresponding drainage area (km^2) for convenience of comparison of results between the Huaxian and Xianyang gauging stations

3.3. Precipitation and temperature data

We download daily total precipitation and daily mean temperature records for 19 meteorological stations over the basin from the National Climate Center of the China Meteorological Administration (source: http://cdc.cma.gov.cn). The areal average daily series of both variables above Huaxian and Xianyang stations are calculated using the Thiessen polygon method (Szolgayova et al., 2014; Thiessen, 1911). The annual average temperature (T) and annual total precipitation (P) over the period 1954-2009 are calculated for each catchment.

Hydrol. Earth Syst. Sci. Discuss., doi:10.5194/hess-2017-259, 2017
Manuscript under review for journal Hydrol. Earth Syst. Sci.
Discussion started: 12 May 2017

4. Results and discussion

4.1. Identification of nonstationarity

Figure 2 shows that the Weihe River basin is characterized by a warm and humid summer (June, July, and August) with low ratio of irrigated diversion, and by a cold and dry winter (December, January, and February) with high ratio of irrigated diversion. The majority of the low flow events in this basin occur in these two seasons and show a bimodal frequency distributions of occurrence with two peaks in February and June, respectively (Fig. 2a). This result implies that the generation of low flows may be influenced by more than one factor such as high ratio of irrigated diversion, high air temperature or lack of precipitation.

<Figure 2>

Overall, four annual minimum streamflow series (AM_1, AM_7, AM_{15} and AM_{30}) in both Huaxian and Xianyang gauging stations show decreasing trends, as indicated by the fitted (dashed) trend lines in Fig. 3. Compared with Huaxian, Xianyang has a larger runoff modulus (the flow per square kilometer) and a larger decrease in annual minimum streamflow series. For example, the decline slope of AM_{30} is -0.0725 ($10^{-4}\ \mathrm{m}^3 \cdot \mathrm{s}^{-1} \cdot \mathrm{km}^{-2}/\mathrm{yr}$) in Huaxian station which is larger than -0.1338 ($10^{-4}\ \mathrm{m}^3 \cdot \mathrm{s}^{-1} \cdot \mathrm{km}^{-2}/\mathrm{yr}$) in Xianyang station.

<Figure 3>

Figure 4 shows the kernel density estimations and time processes of the eight candidate

Hydrol. Earth Syst. Sci. Discuss., doi:10.5194/hess-2017-259, 2017
Manuscript under review for journal Hydrol. Earth Syst. Sci.
Discussion started: 12 May 2017

Hydrology and Earth System Sciences Discussions
Open Access

explanatory variables (Sect. 2.3) reflecting the TCCCs for both Huaxian (H) and Xianyang (X) stations. The results show that these variables have different variation patterns. For example, the mean frequency of precipitation events (λ) has a decreasing trend, while temperature (T) has an increasing trend.

<Figure 4>

The significance of trends in the four annual minimum streamflow series and eight explanatory variables is tested by the Mann-Kendall trend test (Kendall, 1975; Mann, 1945; Yue et al., 2002), and the change-points in these series are detected by the Pettitt's test (Pettitt, 1979). The results in Table 3 show that in both Huaxian and Xianyang stations, the decreasing trends in all the four low-flow series (AM_1, AM_7, AM_{15} and AM_{30}) and two explanatory variables (λ and P), and the increasing trends in T, ET, and AI_{ET} are significant at the 0.05 level (Table 3), but BFI shows no significant trends. However, K and AI_K had significantly decreasing trends only in Huaxian station ($p\text{-}value < 0.05$). The results of change-point detection show that all low-flow series are located at 1968-1971 ($p\text{-}value < 0.05$) except AM_{30} at Xianyang station whose change point is located at 1993 ($p\text{-}value < 0.05$); for the eight candidate explanatory variables, the change points of the variables related to temperature (T, ET, AI_{ET}) in both stations are located at 1990-1993 ($p\text{-}value < 0.05$), the change points of the variables related to precipitation (λ, P) in both stations are close at 1984-1990 ($p\text{-}value \leq 0.186$) and the change points of the variables related to streamflow recession (K, AI_K) in Huaxian station are located at 1968-1971 ($p\text{-}value < 0.05$). However, BFI in both stations and K, AI_K in Xianyang station show no significant change points.

A preliminary attribution analysis is performed using the Pearson correlation matrix to investigate the relations between the annual minimum series and eight candidate explanatory variables. Figure 5 indicates that there are significant linear correlations between the four minimum low-flow series (AM_1, AM_7, AM_{15} and AM_{30}) and all the explanatory variables, with the absolute values of Pearson correlation coefficients larger than 0.27 ($p\text{-}value < 0.05$). These potential physical causes of nonstationarity in low flows are further considered by establishing low-flow nonstationary model with TCCCs in the following section.

<Figure 5>

4.2. Nonstationary frequency analysis models

4.2.1 Single covariate models

Figure 6 presents the AIC values of the three types of models (M2, M1 and M0) fitted for the low flow series (AM_1, AM_7, AM_{15} and AM_{30}). Some interesting results are shown as follows. First, nonstationary models (M2 and M1) have lower AIC values than stationary model (M0), which suggests that nonstationary models are worth considering. Second, for Huaxian, irrespective of the chosen explanatory variables, the distribution type plays an important role in modeling nonstationary low flow series. For example, PIII, GA and WEI distributions in most cases have lower AIC values than LOGNO and GEV distribution. However, for Xianyang, choosing a suitable explanatory variable may be more important than choosing a distribution type. For example, variables t, P, T, and AI_{ET} in most cases have lower AIC values than the other explanatory variables. Finally, in Huaxian, the best M2 models for modeling AM_1, AM_7, AM_{15} and AM_{30} are all found in the M2_AI_K model (using AI_K as an explanatory variable); while in Xianyang, the best M2 models for modeling AM_1, AM_7, AM_{15} and AM_{30} are all found in the M2_K, M2_AI_{ET}, M2_AI_{ET} and M2_T model, respectively. These results indicated that in Huaxian, AI_K is the dominant variable causing nonstationarity in AM_1, AM_7, AM_{15} and AM_{30}; while in Xianyang, the dominant variables causing nonstationarity in AM_1, AM_7, AM_{15} and AM_{30} are K, AI_{ET}, AI_{ET} and T, respectively. Table 4 summarizes the above analysis.

<Figure 6>

Figure 7 shows the diagnostic assessment of the best M2 model (GA_M2 with the optimal explanatory variable) for AM_{30} in both Huaxian and Xianyang stations. The centile curves plots of GA_M2 (Figs. 7a and 7b) show the observed values of AM_{30}, the estimated median and the areas between the 5th and 95th centiles. Figure 7a shows the response relationship between AM_{30}

Hydrol. Earth Syst. Sci. Discuss., doi:10.5194/hess-2017-259, 2017
Manuscript under review for journal Hydrol. Earth Syst. Sci.
Discussion started: 12 May 2017

and AI_K in Huaxian: the increase of AI_K means the smaller magnitude of low-flow events because a high value of AI_K (faster stream recession or fewer rainy days) may lead to faster water loss or less supply. In Fig. 7b, the higher values of T means the smaller magnitude of low flow events, which suggests that T plays an important role in driving low-flow generation in Xianyang. Figs 7c and 7d show that the worm points are within the 95% confidence intervals, thereby indicating a good model fit.

<Figure 7>

4.2.2 Multiple covariate models

Figure 8 shows that the AIC values of stationary model (M0), time covariate model (M1), physical covariate models (M2, M3 and M4 with the corresponding optimal explanatory variables) for AM_1, AM_7, AM_{15} and AM_{30} in both Huaxian and Xianyang stations. For all low flow series, the lowest AIC values are always found in the M4 models, suggesting that it is necessary to consider multiple explanatory variables for nonstationary modeling.

<Figure 8>

A summary of frequency analysis based on five types of models (M0, M1, M2, M3 and M4) for both Huaxian and Xianyang gauging stations is presented in Table 5 and Table 6, respectively. For M4 and M3 models, the relative importance of selected explanatory variables is identified

Hydrol. Earth Syst. Sci. Discuss., doi:10.5194/hess-2017-259, 2017
Manuscript under review for journal Hydrol. Earth Syst. Sci.
Discussion started: 12 May 2017

Hydrology and Earth System Sciences
Open Access
Discussions
EGU

through the stepwise selection method. For instance, for AM_{30} in Xianyang (Table 5), temperature (T) with highest relative importance, followed orderly by P, BFI and K. We can also find that if the candidates are highly correlated, they do not seem to be selected as the explanatory variables at the same time. For example, one of those variables in terms of only air temperature (T), evapotranspiration (ET) and the climate aridity index (AI_{ET}) will appear in a best subset of eight candidates in the final optimum model. This suggests that multicollinearity problem in multiple variables analysis can be reduced, which will help obtain more reliable GLMs parameters for contribution analysis.

The diagnostic assessment of the best M4 model (GA_M4) for AM_{30} at two stations is presented by Fig. 9. The centile curves plots of GA_M4 (Figs. 9a and 9b) show the more sophisticated nonstationary modeling than GA_M2 (Fig 7). When using GA_M4 to model AM_{30} in Huaxian (Fig. 9a), similar to GA_M2, the lower low flows are found to also correspond to high value of AI_K, but GA_M4 are able to identify the more complex variation patterns of low flows through the incorporation of BFI and AI_{ET}. Figures 9c and 9d show that the data points of worm plots of GA_M4 are almost within the 95% confidence intervals, thereby indicating a acceptable model fit.

<Figure 9>

Figure 10 presents the contribution of each selected explanatory variable to $\ln\left(\theta_1^t\right)-\ln\left(\bar{\theta}_1\right)$

in observation year based on GA_M4 for AM_{30} in Huaxian and Xianyang. We can find that for Huaxian, the simulation value of $\ln\left(\theta_1^t\right)$ frequently occur below $\ln\left(\bar{\theta}_1\right)$ during the two periods of about 1970-1982 and 1993-2003, which is in accordance with the observed decrease in AM_{30} of Huaxian station during these periods. In the former period 1970-1982, the largest negative contribution is found in AI_K. In the latter period 1993-2003, the largest negative contribution was found in AI_{ET}. These results suggest that the significant change of AI_K (mainly because of faster streamflow recession after nearly 1971) dominates the decrease in AM_{30} of Huaxian during 1970-1982, while after 1993, the significant change of AI_{ET} (due to decreasing precipitation and increasing evapotranspiration) has a main effect on the decrease in AM_{30} of Huaxian.

4.3. Discussion

The impacts of both human activities and climate change on low flows of the study area of the Weihe basin led to time-varying climate and catchment conditions (TCCCs). Nonstationary modeling for annual low flow series considering TCCCs is clearly different from either the stationary model (M0) or the time covariate model (M1). The result demonstrates that considering multiple drivers (e.g. the variability in catchment conditions), especially in such an artificially influenced river, is necessary for nonstationary modeling of annual low flow series.

In this study area, nonstationary modeling considering TCCCs is supported by the following facts and findings. For human activities, an important milestone representative is the completion and operation of the irrigation system on plateau in Baoji Gorge Irrigation Area since 1971 (Sect. 3.1). The change-point detection test in Sect. 4.1 shows that significant change points of both annual recession constant (K) and low flow series occur exactly in around 1971. This result demonstrates that changes in both K and AM_{30} may involve a consequence of this project. In addition to human activities, climate change also makes a considerable contribution to nonstationarity of low flows, as suggested by nonstationary modeling using TCCCs with stepwise analysis. Actually, climate driving pattern may strengthen after nearly 1990, which is indicated by change-point detection test of both annual mean temperature (T) and annual precipitation (P) as well as the behavior of annual low flow series after nearly 1990. Therefore, the temporal variability in streamflow recession, air temperature and precipitation (the frequency and volume of rain events) should be the main driving factors of generating low flow regimes.

Ignoring the negative impacts of the errors in estimating annual recession constant (K) which are caused by insufficient data points of extracted stream segments at some wet years may lead to the propagation of high errors in annual recession analysis, and accordingly affect the quality of nonstationary frequency analysis when using K as an explanatory variable. Further study will give more reliable estimation of K through improving annual recession analysis.

Hydrol. Earth Syst. Sci. Discuss., doi:10.5194/hess-2017-259, 2017
Manuscript under review for journal Hydrol. Earth Syst. Sci.
Discussion started: 12 May 2017

Hydrology and Earth System Sciences
Discussions
Open Access

5. Conclusion

There is an increasing need to develop an effective nonstationary low-flow frequency model to deal with nonstationarities caused by climate change and time-varying anthropogenic activities. In this study, time-varying climate and catchment conditions (TCCCs) in the Weihe River basin were measured by annual time series of the eight indices, i.e., total precipitation (P), mean frequency of precipitation events (λ), temperature (T), potential evapotranspiration (ET), climate aridity index (AI_{ET}), base-flow index (BFI), recession constant (K), and the recession-related aridity index (AI_K). The nonstationary distribution model was developed using these eight indices as candidate explanatory variables for frequency analysis of time-varying annual low flow series caused by multiple drivers. The main driving forces of the decrease in low flows in the Weihe River include reduced precipitation, warming climate and faster streamflow recession. Therefore, a complex deterioration mechanism resulting from these factors demonstrates that in this arid and semi-arid area, the water resources could be vulnerable to adverse environmental changes, thus portending increasing water shortages. The nonstationary low-flow model considering TCCCs can provide the knowledge of low-flow generation mechanism and give more reliable design of low flows for infrastructure and water supply.

Acknowledgements

The study was financially supported by the National Natural Science Foundation of China (NSFC Grants 51525902 and 51479139), and projects from State Key Laboratory of Water Resources and Hydropower Engineering Science, Wuhan University.

Reference

Akaike, H.: A new look at the statistical model identification, IEEE Transactions on Automatic Control, 19, 716-723, 1974.

Arora, V. K.: The use of the aridity index to assess climate change effect on annual runoff, Journal of Hydrology, 265, 164-177, 2002.

Botter, G., Basso, S., Rodriguez-Iturbe, I., and Rinaldo, A.: Resilience of river flow regimes, Proc Natl Acad Sci U S A, 110, 12925-12930, 2013.

Bradford, M. J. and Heinonen, J. S.: Low Flows, Instream Flow Needs and Fish Ecology in Small Streams, Canadian Water Resources Journal, 33, 165-180, 2008.

Buuren, S. V. and Fredriks, M.: Worm plot: a simple diagnostic device for modelling growth reference curves, Statistics in Medicine, 20, 1259-1277, 2001.

Dobson, A. J. and Barnett, A. G.: An Introduction to Generalized Linear Models, Third Edition, Journal of the Royal Statistical Society, 11, 272-272, 2012.

Du, T., Xiong, L., Xu, C.-Y., Gippel, C. J., Guo, S., and Liu, P.: Return period and risk analysis of nonstationary low-flow series under climate change, Journal of Hydrology, 527, 234-250, 2015.

Dunn, P. K. and Symth, G. K.: Randomized quantile residuals, Journal of Computational and Graphical Statistics, 5, 236-244, 1996.

Giuntoli, I., Renard, B., Vidal, J. P., and Bard, A.: Low flows in France and their relationship to large-scale climate indices, Journal of Hydrology, 482, 105-118, 2013.

Gottschalk, L., Yu, K.-x., Leblois, E., and Xiong, L.: Statistics of low flow: Theoretical derivation of the distribution of minimum streamflow series, Journal of Hydrology, 481, 204-219, 2013.

Guo, D.: An R Package for Implementing Multiple Evapotranspiration Formulations, 2014.

Hall, F. R.: Base flow recessions: A review, Water Resources Research, 4, 973-983, 1968.

Hargreaves, G. H. and Samani, Z. A.: Reference Crop Evapotranspiration From Temperature, 1, 1985.

Hewa, G. A., Wang, Q. J., McMahon, T. A., Nathan, R. J., and Peel, M. C.: Generalized extreme value distribution fitted by LH moments for low-flow frequency analysis, Water Resources Research, 43, n/a-n/a, 2007.

Jiang, C., Xiong, L., Wang, D., Liu, P., Guo, S., and Xu, C.-Y.: Separating the impacts of climate change and human activities on runoff using the Budyko-type equations with time-varying parameters, Journal of Hydrology, 522, 326-338, 2015.

Jiang, C., Xiong, L., Xu, C. Y., and Guo, S.: Bivariate frequency analysis of nonstationary low ‐ flow series based on the time ‐ varying copula, Hydrological Processes, 29, 1521-1534, 2014.

Jones, R. N., Chiew, F. H. S., Boughton, W. C., and Zhang, L.: Estimating the sensitivity of mean annual runoff to climate change using selected hydrological models, Advances in Water Resources, 29, 1419-1429, 2006.

Kam, J. and Sheffield, J.: Changes in the low flow regime over the eastern United States (1962–2011): variability, trends, and attributions, Climatic Change, 135, 639-653, 2015.

Kendall, M. G.: Rank Correlation Methods. , Griffin, Londom, 1975.

Koffler, D. and Laaha, G.: LFSTAT - Low-Flow Analysis in R, Egu General Assembly, 15, 2013.

Hydrol. Earth Syst. Sci. Discuss., doi:10.5194/hess-2017-259, 2017
Manuscript under review for journal Hydrol. Earth Syst. Sci.
Discussion started: 12 May 2017

Kormos, P. R., Luce, C. H., Wenger, S. J., and Berghuijs, W. R.: Trends and sensitivities of low streamflow extremes to discharge timing and magnitude in Pacific Northwest mountain streams, Water Resources Research, 52, 4990-5007, 2016.

Kwon, H.-H., Brown, C., and Lall, U.: Climate informed flood frequency analysis and prediction in Montana using hierarchical Bayesian modeling, Geophysical Research Letters, 35, 2008.

López, J. and Francés, F.: Non-stationary flood frequency analysis in continental Spanish rivers, using climate and reservoir indices as external covariates, Hydrology and Earth System Sciences, 17, 3189-3203, 2013.

Lin, Q. C., Huai-En, L. I., and Xi-Jun, W. U.: Impact of Water Diversion of Baojixia Irrigation Area to the Weihe River Runoff, Yellow River, 2012. 2012.

Liu, D., Guo, S., Lian, Y., Xiong, L., and Chen, X.: Climate-informed low-flow frequency analysis using nonstationary modelling, Hydrological Processes, 29, 2112-2124, 2015.

Mann, H. B.: Nonparametric Tests Against Trend, Econometrica, 13, 245-259, 1945.

Matalas, N. C.: Probability distribution of low flows, U.S. Geological Survey professional Paper, 434-A, 1963.

Milly, P. C. D., Betancourt, J., Falkenmark, M., Hirsch, R. M., Kundzewicz, Z. W., Lettenmaier, D. P., and Stouffer, R. J.: Stationarity Is Dead: Whither Water Management?, Science, 319, 573-574, 2008.

Pettitt, A. N.: A Non-Parametric Approach to the Change-Point Problem, Journal of the Royal Statistical Society, 28, 126, 1979.

Richard, W. K., Marc, B. P., and Philippe, N.: Statistics of extremes in hydrology, Advances in Water Resources, 25, 1287-1304, 2002.

Rigby, R. A. and Stasinopoulos, D. M.: Generalized additive models for location, scale and shape, Appl. Statist., 54, 507-554, 2005.

Roderick, M. L., Sun, F., Lim, W. H., and Farquhar, G. D.: A general framework for understanding the response of the water cycle to global warming over land and ocean, Hydrology & Earth System Sciences Discussions, 10, 15263-15294, 2013.

Sadri, S., Kam, J., and Sheffield, J.: Nonstationarity of low flows and their timing in the eastern United States, Hydrology & Earth System Sciences Discussions, 12, 2761-2798, 2015.

Sawaske, S. R. and Freyberg, D. L.: An analysis of trends in baseflow recession and low-flows in rain-dominated coastal streams of the pacific coast, Journal of Hydrology, 519, 599-610, 2014.

Smakhtin, V. U.: Low flow hydrology： a review, Journal of Hydrology, 2001. 2001.

Stasinopoulos, D. M. and Rigby, R. A.: Generalized additive models for location scale and shape (GAMLSS) in R, Journal of Statistical Software, 23, 2007.

Strupczewski, W. G., Singh, V. P., and Feluch, W.: Non-stationary approach to at-site flood frequency modeling I. Maximum likelihood estimation, Journal of Hydrology, 248, 123-142, 2001.

Szolgayova, E., Parajka, J., Blöschl, G., and Bucher, C.: Long term variability of the Danube River flow and its relation to precipitation and air temperature, Journal of Hydrology, 519, 871-880, 2014.

Tallaksen, L. M.: A review of baseflow recession analysis, Journal of Hydrology, 165, 349-370, 1995.

Tallaksen, L. M., Madsen, H., and Hisdal, H.: Hydrological Drought- Processes and Estimation Methods for Streamflow and Groundwater, Elsevier B.V., the Netherlands, 2004.

Thiessen, A. H.: Precipitation averages for large areas, Monthly Weather Review, 39, 1082-1084, 1911.

Van Loon, A. F. and Laaha, G.: Hydrological drought severity explained by climate and catchment characteristics, Journal of Hydrology, 526, 3-14, 2015.

Venables, W. N. a. R., B. D. (2002) Modern Applied Statistics with S. Fourth edition, 2002. 2002.

Villarini, G., Smith, J. A., and Napolitano, F.: Nonstationary modeling of a long record of rainfall and temperature over Rome, Advances in Water Resources, 33, 1256-1267, 2010.

Villarini, G., Smith, J. A., Serinaldi, F., Bales, J., Bates, P. D., and Krajewski, W. F.: Flood frequency analysis for nonstationary annual peak records in an urban drainage basin, Advances in Water Resources, 32, 1255-1266, 2009.

Villarini, G. and Strong, A.: Roles of climate and agricultural practices in discharge changes in an agricultural watershed in Iowa, Agriculture, Ecosystems & Environment, 188, 204-211, 2014.

WMO: Mannual on Low-fow Estimation and Prediction. WMO-No.1029, Switzerland, 2009.

Xiong, L., Du, T., Xu, C.-Y., Guo, S., Jiang, C., and Gippel, C. J.: Non-Stationary Annual Maximum Flood Frequency Analysis Using the Norming Constants Method to Consider Non-Stationarity in the Annual Daily Flow Series, Water Resources Management, 29, 3615-3633, 2015.

Yu, K.-x., Xiong, L., and Gottschalk, L.: Derivation of low flow distribution functions using copulas, Journal of Hydrology, 508, 273-288, 2014.

Yue, S., Pilon, P., and Cavadias, G.: Power of the Mann–Kendall and Spearman's rho tests for detecting monotonic trends in hydrological series, Journal of Hydrology, 259, 254-271, 2002.

Zhang, Y. P.: Economical water-use mode research of Baoji Gorge Irrigation Area based on WebGIS. Chinese, 2008. 2008.

Figure

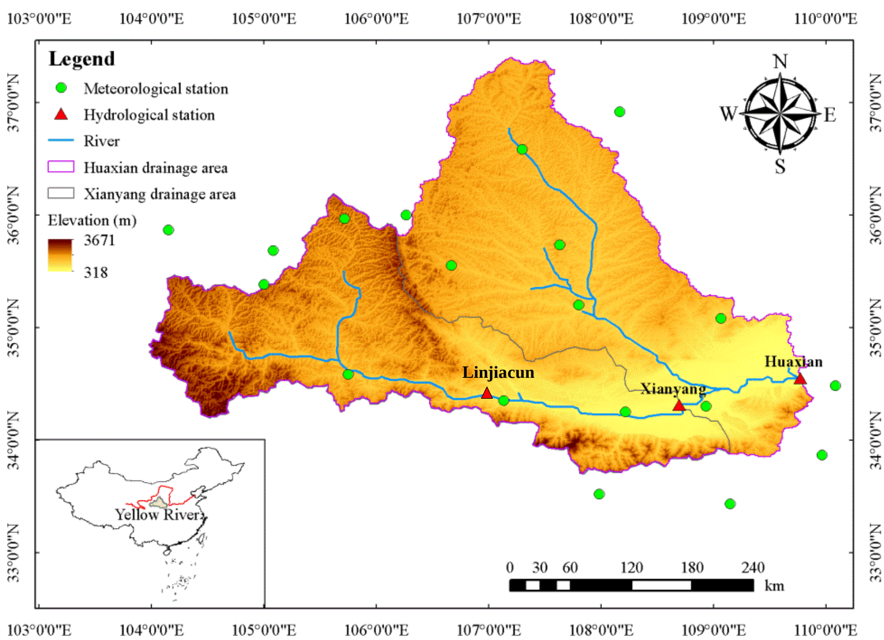

Figure 1. Location, topography, hydro-meteorological stations and river systems of the Weihe River basin.

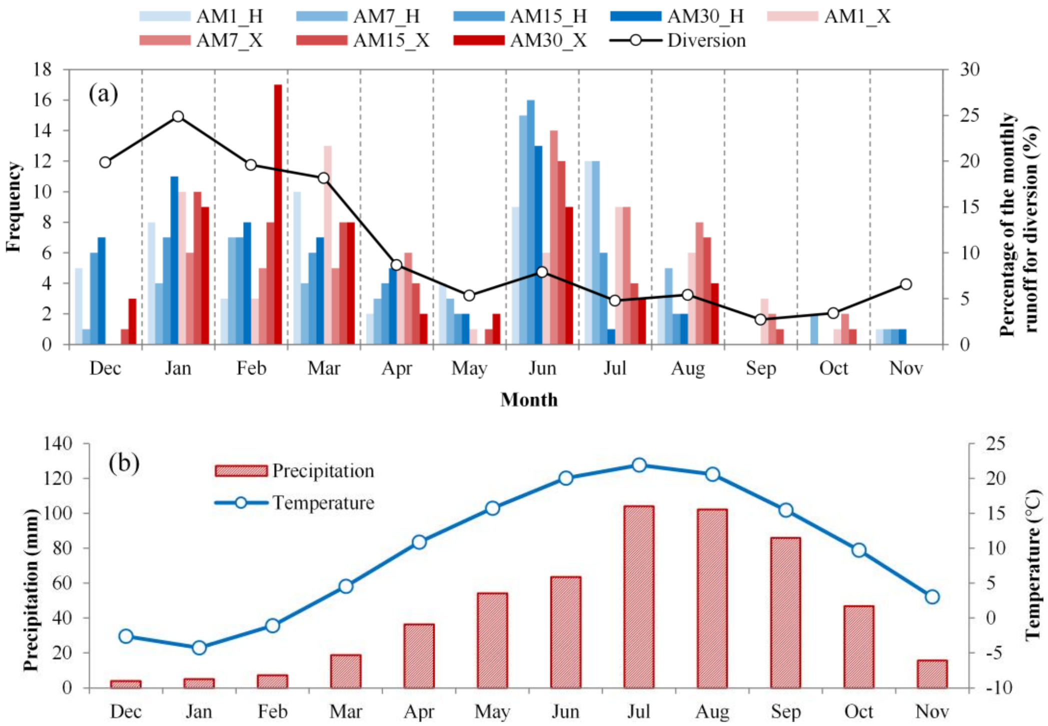

Figure 2. Overview of annual low flows and important environment factors using mean monthly data. (a) is frequency distributions of the occurrence time of the annual minimum flows with four durations at Huaxian (H) and Xianyang (X); the black line is mean monthly diversion (1980 to 2005) in Baoji Gorge area. (b) Mean monthly precipitation and temperature from 1954 to 2009.

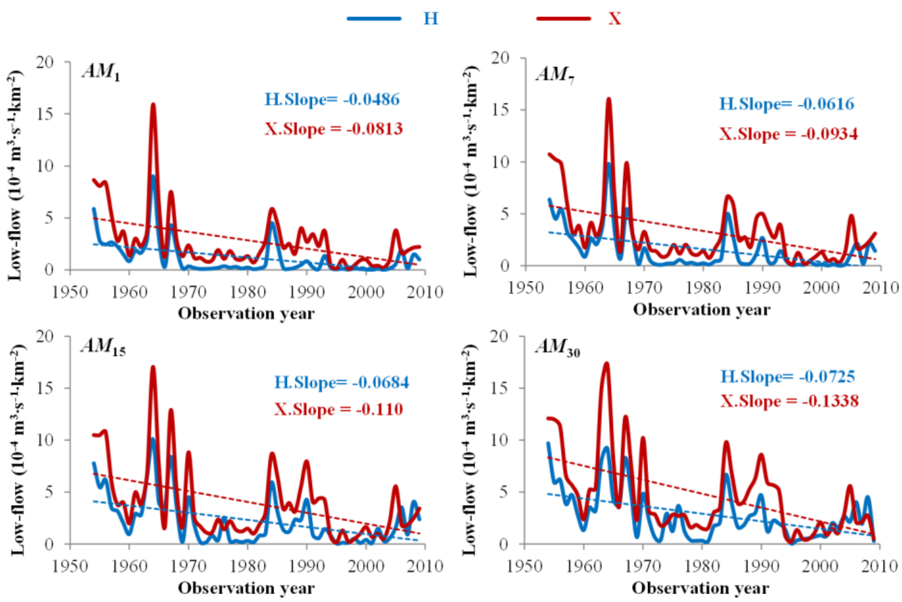

Figure 3. The annual minimum low flows and fitted trend lines in both Huaxian (H) and Xianyang (X) gauging stations.

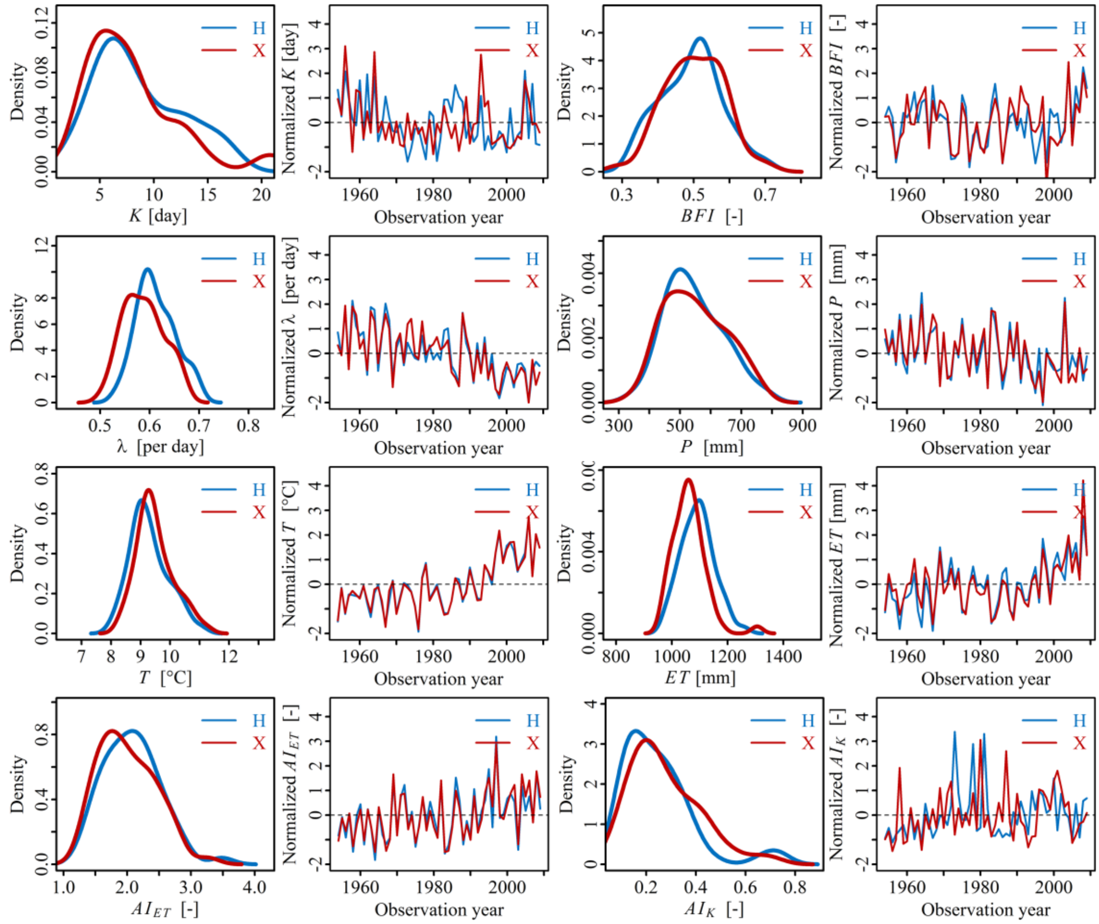

Figure 4. Frequency distributions (using the kernel density estimations) and annual series of eight candidate explanatory variables in both Huaxian (H) and Xianyang (X) stations.

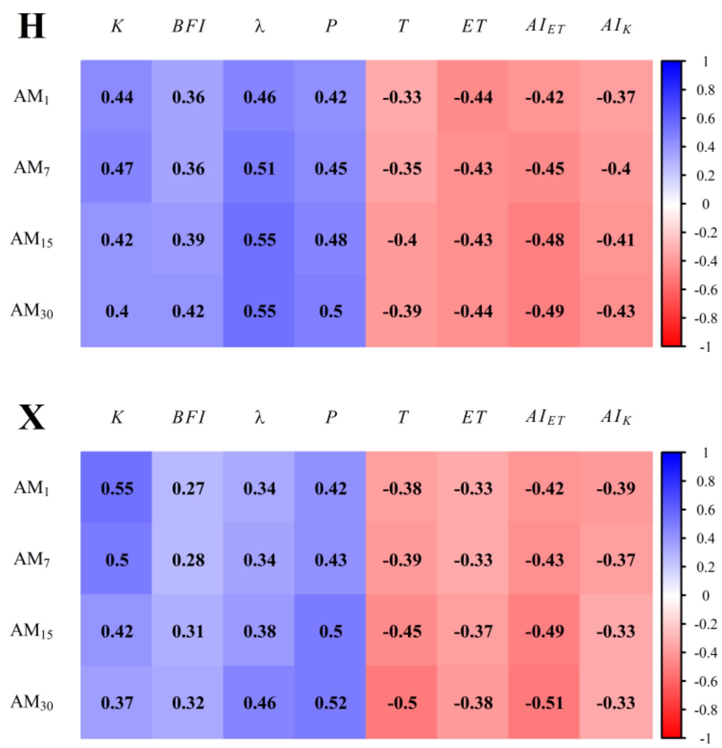

Figure 5. The Pearson correlation coefficients matrix between the annual minimum flow series and eight candidate explanatory variables in Huaxian (H) and Xianyang (X) stations; the darker color intensity represents a higher level of correlation (blue indicates positive correlation, and red indicates negative correlations).

Hydrol. Earth Syst. Sci. Discuss., doi:10.5194/hess-2017-259, 2017
Manuscript under review for journal Hydrol. Earth Syst. Sci.
Discussion started: 12 May 2017

Hydrology and Earth System Sciences Open Access
Discussions

H

		LOGNO	PIII	GEV	WEI	GA	AIC
AM_1	M0_none	112.4	112.9	114.3	108.6	110.9	114.3
	M1_t	94.8	97.0	90.3	94.4	97.0	
	M2_K	102.5	96.7	101.5	95.4	96.7	
	M2_BFI	103.4	99.2	97.6	96.7	99.2	
	M2_λ	99.9	99.1	97.8	96.9	99.1	
	M2_P	106.9	97.9	104.5	97.2	97.9	
	M2_T	101.6	102.8	99.9	100.5	102.8	
	M2_ET	101.5	99.9	100.5	98.3	99.9	
	M2_AI_{ET}	104.8	96.8	103.0	95.8	96.8	
	M2_AI_K	103.6	95.8	101.8	95.0	95.8	90.3

OPTIPAL MODEL: AIC(GEV, t)= 90.3

		LOGNO	PIII	GEV	WEI	GA	AIC
AM_7	M0_none	151.8	155.0	158.2	153.5	155.2	158.2
	M1_t	134.7	138.5	137.9	139.1	140.7	
	M2_K	139.9	138.3	146.3	139.7	140.5	
	M2_BFI	141.8	141.5	146.1	142.1	143.7	
	M2_λ	137.7	139.4	142.4	140.3	141.6	
	M2_P	144.6	138.5	147.4	140.4	140.7	
	M2_T	141.6	144.6	144.4	145.2	146.7	
	M2_ET	141.6	142.6	147.0	143.7	144.8	
	M2_AI_{ET}	142.7	137.9	146.2	139.5	140.0	
	M2_AI_K	139.9	135.7	140.7	137.7	138.0	134.7

OPTIPAL MODEL: AIC(PIII, t)= 134.7

		LOGNO	PIII	GEV	WEI	GA	AIC
AM_{15}	M0_none	211.9	203.6	222.2	209.0	209.0	222.2
	M1_t	200.6	190.2	210.1	197.5	197.4	
	M2_K	199.9	190.7	208.0	198.0	198.0	
	M2_BFI	200.7	190.4	209.3	197.7	197.7	
	M2_λ	197.6	188.3	204.7	195.4	195.4	
	M2_P	200.6	187.6	210.3	195.0	194.9	
	M2_T	201.8	193.5	209.0	200.7	200.8	
	M2_ET	202.3	192.7	210.6	199.9	199.9	
	M2_AI_{ET}	199.4	187.3	209.0	194.6	194.5	
	M2_AI_K	197.5	184.2	205.7	192.3	192.2	184.2

OPTIPAL MODEL: AIC(PIII, AI_K)= 184.2

		LOGNO	PIII	GEV	WEI	GA	AIC
AM_{30}	M0_none	241.4	237.3	244.1	236.5	236.3	244.1
	M1_t	233.0	225.4	233.5	225.4	225.5	
	M2_K	230.1	224.9	232.6	225.1	225.0	
	M2_BFI	226.2	223.5	228.5	224.0	223.5	
	M2_λ	228.5	221.4	227.1	221.1	221.1	
	M2_P	229.0	220.9	228.4	220.6	220.6	
	M2_T	233.4	227.2	232.2	227.7	227.5	
	M2_ET	232.9	226.2	233.3	226.4	226.4	
	M2_AI_{ET}	228.1	220.5	227.5	220.1	220.1	
	M2_AI_K	224.5	217.5	220.8	217.7	217.4	217.4

OPTIPAL MODEL: AIC(GA, AI_K)=217.4

X

		LOGNO	PIII	GEV	WEI	GA	AIC
AM_1	M0_none	227.2	226.5	228.0	227.2	226.3	228.0
	M1_t	211.1	210.6	209.5	211.5	209.9	
	M2_K	215.4	211.4	212.9	212.2	210.7	
	M2_BFI	220.8	217.0	218.8	218.9	217.7	
	M2_λ	217.2	216.1	218.6	217.7	216.5	
	M2_P	215.6	211.9	215.6	212.9	211.5	
	M2_T	211.9	212.8	211.5	214.4	212.7	
	M2_ET	217.0	216.6	214.9	218.4	217.1	
	M2_AI_{ET}	213.6	211.3	214.1	212.3	210.8	
	M2_AI_K	218.2	214.0	217.4	215.2	214.0	209.5

OPTIPAL MODEL: AIC(GEV, t)= 209.5

		LOGNO	PIII	GEV	WEI	GA	AIC
AM_7	M0_none	243.5	243.8	245.8	245.1	244.1	245.8
	M1_t	227.9	228.2	228.0	229.7	227.9	
	M2_K	233.1	230.6	232.5	232.3	230.7	
	M2_BFI	235.9	234.2	236.2	236.8	235.4	
	M2_λ	233.8	233.3	236.8	235.5	234.2	
	M2_P	232.3	229.0	233.6	230.4	229.0	
	M2_T	229.1	230.1	230.5	232.2	230.3	
	M2_ET	234.4	234.0	234.7	236.4	235.0	
	M2_AI_{ET}	230.6	228.5	232.6	230.0	228.4	
	M2_AI_K	235.6	232.2	236.3	234.1	232.8	227.9

OPTIPAL MODEL: AIC(GA, t)= 227.9

		LOGNO	PIII	GEV	WEI	GA	AIC
AM_{15}	M0_none	269.9	269.3	273.3	270.0	269.3	273.3
	M1_t	254.5	253.5	256.1	254.6	253.4	
	M2_K	262.0	259.0	262.9	260.8	259.8	
	M2_BFI	261.6	258.6	262.7	260.5	259.5	
	M2_λ	259.3	257.4	263.4	259.0	258.1	
	M2_P	256.2	251.6	258.9	252.4	251.4	
	M2_T	254.3	253.5	256.7	255.0	253.6	
	M2_ET	260.6	258.5	262.7	260.2	259.3	
	M2_AI_{ET}	254.7	251.3	258.2	252.1	251.0	
	M2_AI_K	263.1	259.2	264.8	261.0	260.2	251.0

OPTIPAL MODEL: AIC(GA, AI_{ET})= 251.0

		LOGNO	PIII	GEV	WEI	GA	AIC
AM_{30}	M0_none	290.7	290.6	293.4	290.8	289.8	293.4
	M1_t	271.6	270.4	271.5	271.8	270.1	
	M2_K	284.0	281.1	284.1	282.9	281.7	
	M2_BFI	282.3	278.8	284.1	280.3	279.3	
	M2_λ	276.9	274.7	279.6	276.0	274.8	
	M2_P	275.1	271.1	277.0	272.1	270.9	
	M2_T	270.8	270.3	271.1	272.1	270.1	
	M2_ET	280.9	278.3	282.1	279.9	278.7	
	M2_AI_{ET}	273.7	270.5	276.0	271.6	270.2	
	M2_AI_K	283.9	279.9	284.0	281.5	280.5	270.1

OPTIPAL MODEL: AIC(GA, T)= 270.1

Figure 6. Comparisons among M0, M1 and M2 based on the AIC values for the four observed low-flow series in Huaxian (H) at left panel and Xianyang (X) at right panel; darker red color represents a higher goodness of fit.

Hydrol. Earth Syst. Sci. Discuss., doi:10.5194/hess-2017-259, 2017
Manuscript under review for journal Hydrol. Earth Syst. Sci.
Discussion started: 12 May 2017

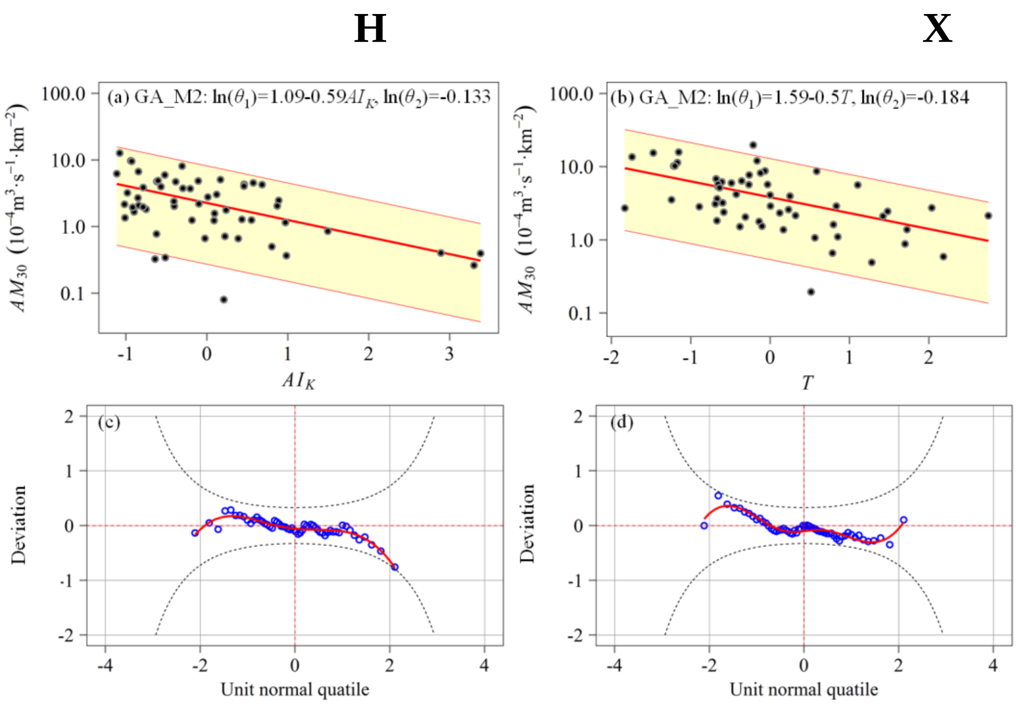

Figure 7. Performance assessments of the best M2 model (GA_M2) for AM_{30} in Huaxian (H) at left panel and Xianyang (X) at right panel. (a) and (b) are the centile curves plots of GA_M2 (red lines represent the centile curves estimated by GA_M2; the 50th centile curves are indicated by thick red; the yellow-filled areas are between the 5th and 95th centile curves; the black points indicate the observed series); (c) and (d) are the worm plots of GA_M2 for the goodness-of-fit test; a reasonable model fit should have the data points fall within the 95% confidence intervals (between the two red dashed curves).

607

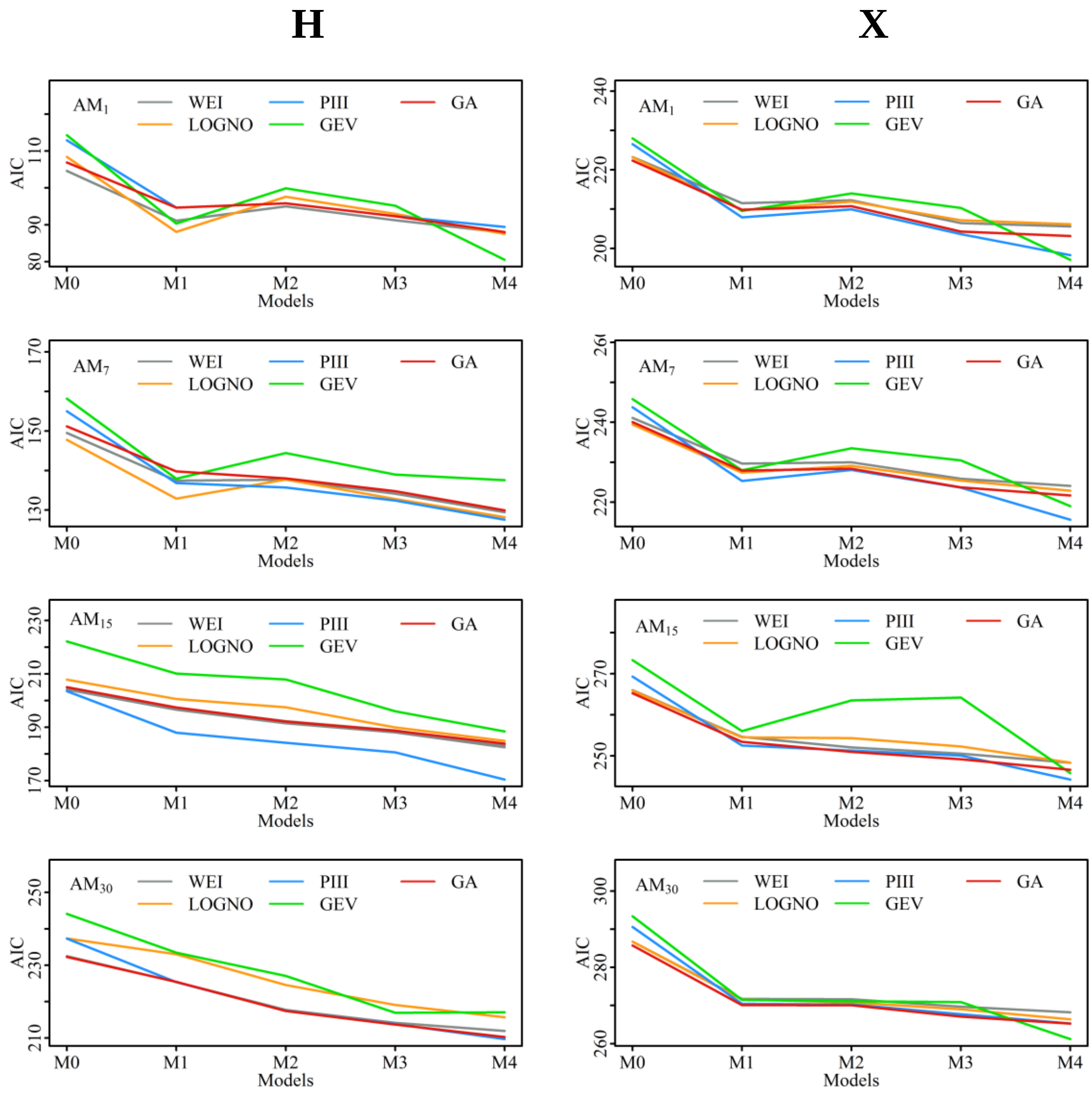

608 Figure 8. Comparisons among stationary model (M0), time covariate model (M1) and physical

609 covariate models (M2, M3, M4 with the corresponding optimal explanatory variables) in Huaxian

610 (H) at left panel) and Xianyang (X) at right panel.

611

612

Hydrology and Earth System Sciences
Open Access
Discussions

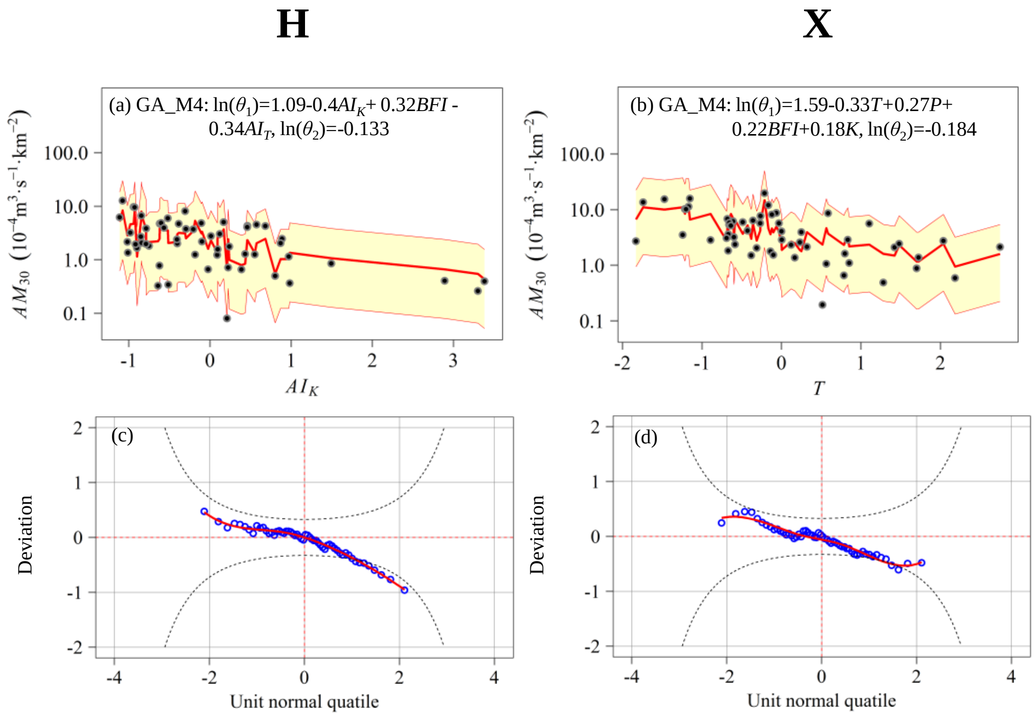

Figure 9. Performance assessments of the best M4 model (GA_M4) for AM_{30} in Huaxian (H) at left panel and Xianyang (X) at right panel. (a) and (b) are the centile curves plots of GA_M4 (red lines represent the centile curves estimated by GA_M4; the 50th centile curves are indicated by thick red; the yellow-filled areas are between the 5th and 95th centile curves; the filled black points indicate the observed series); (c) and (d) are the worm plots of GA_M4 for the goodness-of-fit test; A reasonable model fit should have the data points fall within the 95% confidence intervals (between the two red dashed curves).

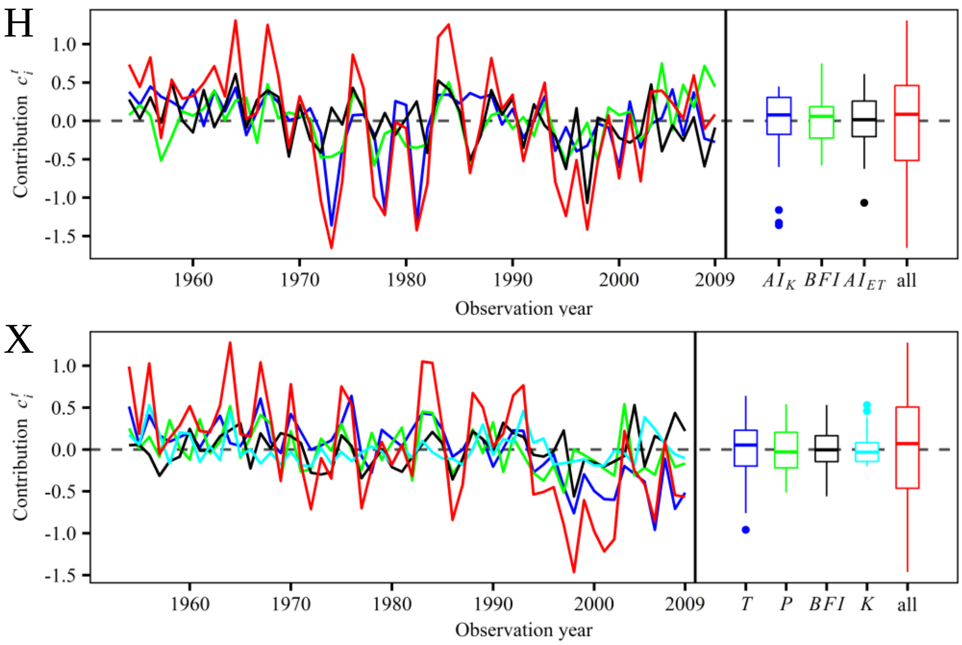

Figure 10. Contribution of selected explanatory variables to $\ln\left(\theta_1^t\right)-\ln\left(\bar{\theta}_1\right)$ in different periods based on GA_M4.

Table

Table 1. The probability density functions and moments (the mean and variance) for the candidate distributions in this study.

Distributions	Probability density function	Distribution moments
Pearson-III	$f_Y\left(y\mid\theta_1,\theta_2,\theta_3\right)=\dfrac{\left(y-\theta_3\right)^{1/\theta_2^2-1}}{\Gamma\left(1/\theta_2^2\right)\left(\theta_1\theta_2^2\right)^{1/\theta_2^2}}\exp\left(-\dfrac{y-\theta_3}{\theta_1\theta_2^2}\right)$ $y>\theta_3,\theta_3>0,\theta_1>0,\theta_2>0$	$E\left[Y\right]=\theta_1+\theta_3$ $Var\left[Y\right]=\theta_1^2\theta_2^2$
Gamma	$f_Y\left(y\mid\theta_1,\theta_2\right)=\dfrac{\left(y\right)^{1/\theta_2^2-1}}{\Gamma\left(1/\theta_2^2\right)\left(\theta_1\theta_2^2\right)^{1/\theta_2^2}}\exp\left(-\dfrac{y}{\theta_1\theta_2^2}\right)$ $y>0,\theta_1>0,\theta_2>0$	$E\left[Y\right]=\theta_1$ $Var\left[Y\right]=\theta_1^2\theta_2^2$
Weibull	$f_Y\left(y\mid\theta_1,\theta_2\right)=\left(\dfrac{\theta_2}{\theta_1}\right)\left(\dfrac{y}{\theta_1}\right)^{\theta_2-1}\exp\left(-\left(\dfrac{y}{\theta_1}\right)^{\theta_2}\right)$ $y>0,\theta_1>0,\theta_2>0$	$E\left[Y\right]=\theta_1\Gamma\left(1+1/\theta_2\right)$ $Var\left[Y\right]=\theta_1^2\left[\Gamma\left(1+\dfrac{2}{\theta_2}\right)-\Gamma^2\left(1+\dfrac{1}{\theta_2}\right)\right]$
Lognormal	$f_Y\left(y\mid\theta_1,\theta_2\right)=\dfrac{1}{y\theta_2\sqrt{2\pi}}\exp\left\{-\dfrac{\left[\log\left(y\right)-\theta_1\right]^2}{2\theta_2^2}\right\}$ $y>0,\theta_2>0$	$E\left[Y\right]=w^{1/2}e^{\theta_1}$ $Var\left[Y\right]=w\left(w-1\right)e^{2\theta_1}$ $w=\exp\left(\theta_2^2\right)$
GEV	$f_Y\left(y\mid\theta_1,\theta_2,\theta_3\right)=\dfrac{1}{\theta_2}\left[1+\theta_3\left(\dfrac{y-\theta_1}{\theta_2}\right)\right]^{-1/\theta_3-1}\exp\left\{-\left[1+\theta_3\left(\dfrac{y-\theta_1}{\theta_2}\right)\right]^{-1/\theta_3}\right\}$ $-\infty<\theta_1<\infty,\theta_2>0,-\infty<\theta_3<\infty$	$E\left[Y\right]=\theta_1-\dfrac{\theta_2}{\theta_3}+\dfrac{\theta_2}{\theta_3}\eta_1$ $Var\left[Y\right]=\theta_2^2\left(\eta_2-\eta_1^2\right)/\theta_3^2$ $\eta_m=\Gamma\left(1-m\theta_3\right)$

Hydrol. Earth Syst. Sci. Discuss., doi:10.5194/hess-2017-259, 2017
Manuscript under review for journal Hydrol. Earth Syst. Sci.
Discussion started: 12 May 2017

Table 2. Description of the developed nonstationary models using time or the indices of TCCCs as explanatory variables.

Model category	Codes	Distribution					Description	
		GA	WEI	LOGNO	PIII	GEV	Variable category	The numbers of variables
Stationary	M0	GA_M0	WEI_M0	LOGNO_M0	PIII_M0	GEV_M0	-	Zero
Nonstationary	M1	GA_M1	WEI_M1	LOGNO_M1	PIII_M1	GEV_M1	Time	One
	M2	GA_M2	WEI_M2	LOGNO_M2	PIII_M2	GEV_M2	TCCCs	One
	M3	GA_M3	WEI_M3	LOGNO_M3	PIII_M3	GEV_M3	TCCCs	Two
	M4	GA_M4	WEI_M4	LOGNO_M4	PIII_M4	GEV_M4	TCCCs	Identified by the stepwise selection

Hydrol. Earth Syst. Sci. Discuss., doi:10.5194/hess-2017-259, 2017
Manuscript under review for journal Hydrol. Earth Syst. Sci.
Discussion started: 12 May 2017

Hydrology and Earth System Sciences Discussions
Open Access EGU

Table 3. The results of trend test and change-point detection for the four low flow series and eight candidate explanatory variables in Huaxian and Xianyang stations.

Station	Variable	Mann-Kendall test		Pettitt's test	
		S	*p-value*	Change point	*p-value*
Huaxian	AM_1	-564	6.91E-05(***)	1968	1.34E-03(**)
	AM_7	-560	7.79E-05(***)	1968	1.44E-03(**)
	AM_{15}	-438	2.01E-03(**)	1971	4.85E-03(**)
	AM_{30}	-378	7.71E-03(**)	1971	9.96E-03(**)
	K	-312	2.79E-02(*)	1968	8.11E-02(.)
	BFI	52	7.19E-01( )	1998	3.88E-01( )
	λ	-632	8.20E-06(***)	1984	3.02E-04(***)
	P	-292	3.97E-02(*)	1985	1.86E-01( )
	T	752	1.11E-07(***)	1993	8.17E-06(***)
	ET	548	1.11E-04(***)	1993	1.98E-03(**)
	AI_{ET}	384	6.79E-03(**)	1990	6.03E-02(.)
	AI_K	376	8.04E-03(**)	1971	3.60E-02(*)
Xianyang	AM_1	-517	2.65E-04(***)	1968	2.2E-03(**)
	AM_7	-483	6.58E-04(***)	1970	2.5E-03(**)
	AM_{15}	-474	8.29E-04(***)	1971	2.2E-03(**)
	AM_{30}	-570	5.78E-05(***)	1993	4.5E-04(***)
	K	-210	1.39E-01( )	1966	2.03E-01( )
	BFI	64	6.56E-01( )	2003	8.65E-01( )
	λ	-652	4.21E-06(***)	1984	6.00E-05(***)
	P	-414	3.51E-03(**)	1990	1.45E-02(*)
	T	724	3.22E-07(***)	1993	5.41E-06(***)
	ET	372	8.74E-03(**)	1993	3.01E-03(**)
	AI_{ET}	454	1.37E-03(**)	1993	8.82E-03(**)
	AI_K	290	4.11E-02(*)	1968	1.63E-01( )

Signif. codes: 0 '***' 0.001 '**' 0.01 '*' 0.05 '.' 0.1 ' ' 1

Hydrol. Earth Syst. Sci. Discuss., doi:10.5194/hess-2017-259, 2017
Manuscript under review for journal Hydrol. Earth Syst. Sci.
Discussion started: 12 May 2017

Table 4. The results of M2 models for modeling low-flow series in Huaxian and Xianyang stations.

Station	Series	Optimal variable	Optimal distribution	AIC	Distribution parameters		
					$\ln(\theta_1)$	$\ln(\theta_2)$	θ_3
Huaxian	AM_1	AI_K	WEI	95.0	$-0.19-0.72AI_K$	-0.418	-
	AM_7	AI_K	PIII	135.7	$0.43-0.76AI_K$	0.219	0.007
	AM_{15}	AI_K	PIII	184.2	$0.83-0.75AI_K$	0.105	0.069
	AM_{30}	AI_K	GA	217.4	$1.09-0.59AI_K$	-0.133	-
Xianyang	AM_1	K	GA	210.7	$1.00+0.40K$	-0.118	-
	AM_7	AI_{ET}	GA	228.4	$1.17-0.45AI_{ET}$	-0.139	-
	AM_{15}	AI_{ET}	GA	251.0	$1.39-0.49AI_{ET}$	-0.139	-
	AM_{30}	T	GA	270.1	$1.59-0.50T$	-0.184	-

Table 5. The summary of frequency analysis for four annual low flow series of Huaxian.

Series	Model codes	Optimal variable	AIC	Distribution parameters		
				$\ln(\theta_1)$	$\ln(\theta_2)$	θ_3
AM_1	WEI_M0	-	104.6	-0.19	-0.418	-
	WEI_M1	t	91.1	-0.19-0.84t	-0.418-0.30t	-
	WEI_M2	AI_K	95.0	-0.19-0.72 AI_K	-0.418	-
	WEI_M3	AI_K, BFI	91.3	-0.19-0.58 AI_K +0.55BFI	-0.418	-
	WEI_M4	AI_K, BFI, ET, λ	87.9	-0.19-0.39 AI_K +0.61BFI-0.54ET	-0.418+0.27λ	-
AM_7	PIII_M0	-	155.0	0.43	0.219	0.007
	PIII_M1	t	136.8	0.43-0.59t	0.219+0.19t	0.007
	PIII_M2	AI_K	135.7	0.43-0.76AI_K	0.219	0.007
	PIII_M3	AI_K, BFI	132.4	0.43-0.65AI_K +0.48BFI	0.219	0.007
	PIII_M4	AI_K, BFI, AI_{ET}, λ, P	127.5	0.43-0.62AI_K +0.57BFI-0.60AI_{ET}	0.219-0.32λ-0.30 AI_K +0.21P	0.007
AM_{15}	PIII_M0	-	203.5	0.83	0.105	0.069
	PIII_M1	t	188.0	0.83-0.46t	0.105+0.208t	0.069
	PIII_M2	AI_K	184.2	0.83-0.75AI_K	0.105	0.069
	PIII_M3	AI_K, BFI	180.6	0.83-0.65AI_K +0.43BFI	0.105	0.069
	PIII_M4	AI_K, BFI, λ, K	170.4	0.83-0.70AI_K +0.42BFI	0.105-0.36λ-0.71 AI_K -0.43K	0.069
AM_{30}	GA_M0	-	232.3	1.09	-0.133	-
	GA_M1	t	225.5	1.09-0.32t	-0.133	-
	GA_M2	AI_K	217.4	1.09-0.59AI_K	-0.133	-
	GA_M3	AI_K, BFI	213.7	1.09-0.5AI_K +0.32BFI	-0.133	-
	GA_M4	AI_K, BFI, AI_T	211.1	1.09-0.4AI_K+0.32BFI -0.34AI_T	-0.133	-

Hydrol. Earth Syst. Sci. Discuss., doi:10.5194/hess-2017-259, 2017
Manuscript under review for journal Hydrol. Earth Syst. Sci.
Discussion started: 12 May 2017

Hydrology and Earth System Sciences
Open Access
Discussions

Table 6. The summary of frequency analysis for four annual low flow series of Xianyang.

Series	Model codes	Optimal variable	AIC	Distribution parameters	
				$\ln(\theta_1)$	$\ln(\theta_2)$
AM_1	GA_M0	-	222.3	1.0	-0.118
	GA_M1	t	209.9	$1.0-0.44t$	-0.118
	GA_M2	K	210.7	$1.0+0.4K$	-0.118
	GA_M3	K, T	204.3	$1.0+0.37K-0.38T$	-0.118
	GA_M4	K, T, BFI, λ	203.2	$1.0+0.33K-0.32T+0.27BFI$	$-0.118-0.17\lambda$
AM_7	GA_M0	-	240.1	1.17	-0.139
	GA_M1	t	227.9	$1.17-0.42t$	-0.139
	GA_M2	AI_{ET}	228.4	$1.17-0.45AI_{ET}$	-0.139
	GA_M3	AI_{ET}, K	223.7	$1.17-0.38AI_{ET}+0.31K$	-0.139
	GA_M4	AI_{ET}, K, BFI, λ	221.7	$1.17-0.31AI_{ET}+0.3K+0.28BFI$	$-0.139-0.2\lambda$
AM_{15}	GA_M0	-	265.3	1.39	-0.139
	GA_M1	t	253.4	$1.39-0.43t$	-0.139
	GA_M2	AI_{ET}	251.0	$1.39-0.49AI_{ET}$	-0.139
	GA_M3	AI_{ET}, K	249.2	$1.39-0.45AI_{ET}+0.24K$	-0.139
	GA_M4	AI_{ET}, K, BFI, λ	246.6	$1.39-0.36AI_{ET}+0.23K+0.32BFI$	$-0.139-0.21\lambda$
AM_{30}	GA_M0	-	285.8	1.59	-0.184
	GA_M1	t	270.1	$1.59-0.48t$	-0.184
	GA_M2	T	270.1	$1.59-0.5T$	-0.184
	GA_M3	T, P	267.1	$1.59-0.34T+0.32P$	-0.184
	GA_M4	T, P, BFI, K	265.4	$1.59-0.33T+0.27P+0.22BFI+0.18K$	-0.184